Supporting Information

Assembling silver clusters-based organic frameworks for higher-performance hypergolic properties

Chao Wang,[†] Ya-Jie Wang, [†] Chun-Lin He,[‡] Qian-You Wang,*[,†] and Shuang-Quan Zang[†]

[†]Henan Key Laboratory of Crystalline Molecular Functional Materials, Henan International Joint Laboratory of Tumor Theranostical Cluster Materials, Green Catalysis Center and College of Chemistry, Zhengzhou University. Zhengzhou 450001, China

[‡]Chongqing Innovation Center, Beijing Institute of Technology, Chongqing 401120, China

*E-mail:qianyouwang@zzu.edu.cn

Section S1: Materials and Methods

Materials and Reagents

All chemicals and solvents obtained from suppliers were used without further purification.

Measurements

Single-crystal X-ray diffraction (SCXRD) was performed on a Rigaku XtaLAB Pro diffractometer with Cu Kα radiation (λ = 1.54184 Å). Fourier transform infrared attenuated total reflection (FTIR-ATR) spectra were recorded in the range of 400-4000 cm^{-1} on a Bruker ALPHA spectrometer. Powder X-ray diffraction (PXRD) was performed on a Rigaku D/Max-2500PC X-ray diffractometer with a Cu sealed tub (λ = 1.54178 Å). Thermogravimetric analysis (TGA) was performed on an SDT 2960 thermal analyser from room temperature to 600 °C at a heating rate of 10 °C/min. High purity N_2 (99.99%) was applied throughout the TG analysis under N_2 atmosphere. When performed thermal analysis under O_2 atmosphere, the ratio between O_2 and N_2 is 3:2. Elemental analyses were carried out on a Vario EL III CHNOS elemental analyser. Bomb calorimetry was performed in a high-pressure bomb calorimeter (IDEA science BCA 500). In a typical experiment, 0.2 g of material was put into the crucible to be oxidized in the bomb under 30 bar of oxygen, and pellets of benzoic acid were used as a reference. Impact sensitivity was tested on the BAM Fall Hammer Impact Sensitivity Tester BFH 12 produced by OZM Research. Solid samples were placed directly into the open impact device, and a standard hammer drop test, in which a 2.7 kg hardened steel weight was released from a height of up to 2.1 m (corresponding to impact of approximately 50 J) was performed. No detonation or ignition was observed for any of the samples, even at an impact of 50 J. Specific impulse data were calculated by means of ExplO5 (version 6.05.04) software.

Caution!

All compounds are energetic materials that tend to explode under certain conditions. Thus, all the hypergolic testing in this study was performed in a fume hood, and anti-cutting gloves, leather coats, face shields and earplugs were used.

Section S2: Synthesis of 1-Propargylimidazole (PIm), ZZU-361, ZZU-362 and ZZU-363

Synthesis of PIm and Ag-precursor

The ligand PIm was prepared by a literature method with slight modifications.[1] A 50 mL round-bottom flask equipped with a magnetic stirring bar was charged with imidazole (0.953 g, 14.00 mmol), NaOH (0.560 g, 14.00 mmol) and THF (30 mL). The resulting mixture was stirred at 50 °C for 1 h and then cooled to 25 °C. Subsequently, 3-bromopropyne (1.856 g, 30.80 mmol) was added dropwise, and the solution was stirred for another 10 h. After filtration, concentration, washing, drying and purification on a silica gel column, the compound (PIm) was obtained. Yield: 0.964 g (65.0 %).

The Ag precursor was prepared from PIm and Ag_2O by a common method described in a previous article[2].

Synthesis of ZZU-361

The Ag precursor (11 mg, 0.05 mmol) and CF_3COOAg (11 mg, 0.05 mmol) were dissolved in a mixed solvent of CH_3OH and DMF (1:2, 6 mL). Then, CF_3COOH (10 μL) was added, and the reaction mixture was stirred for 12 h in the absence of light. The reaction solvent was filtered. The filtrate was slowly evaporated in air for approximately 3 days to give a colourless block-like crystal of ZZU-361. Yield: 45.5%. Elemental analysis for $Ag_{12}(PIm)_6(CF_3COO)_6(DMF)_2$: calcd. C, 23.58%; H, 1.61%; N, 7.13%; found: C, 23.45%; H, 1.91%; N, 7.78%.

Synthesis of ZZU-362

The Ag precursor (11 mg, 0.05 mmol) was added to a mixed solvent of DMF/CH_3OH/CH_3CN (6 mL, 1:1:1). Then, CF_3COOAg (11 mg, 0.05 mmol) and CF_3COOH (10 μL) were added to the above mixture. The solution was stirred for approximately 20 min at room temperature and then filtered. A colourless tiny block-like crystal of ZZU-362 was prepared by slowly evaporating the filtrate in a dark environment at room temperature for approximately ten days. Yield: 50.3%. Elemental analysis for $[Ag_{14}(PIm)_8(CF_3COO)_6]$ • (DMF)(MeOH): calcd. C, 24.52%; H, 1.77%; N, 7.59%; found: C, 24.33%; H, 1.59%; N, 7.29%.

Synthesis of ZZU-363

A 1 mL EtOH solution containing $Cu(NO_3)_2$ (24 mg, 0.1 mmol) was added to the abovementioned solution of ZZU-361. Then, the solution turned blue and was stirred overnight and then filtered. The filtrate was slowly evaporated in air and allowed to stand for several days, and a colourless crystal of ZZU-363 was deposited. Yield: 40.1%. Elemental analysis for $Ag_{16}(C_6N_2H_5)_8(NO_3)_8$: calcd. C, 18.82%; H, 1.31%; N, 10.98%; found: C, 19.76%; H, 1.54%; N, 10.75%.

Section S3: Characterization of ligand and materials

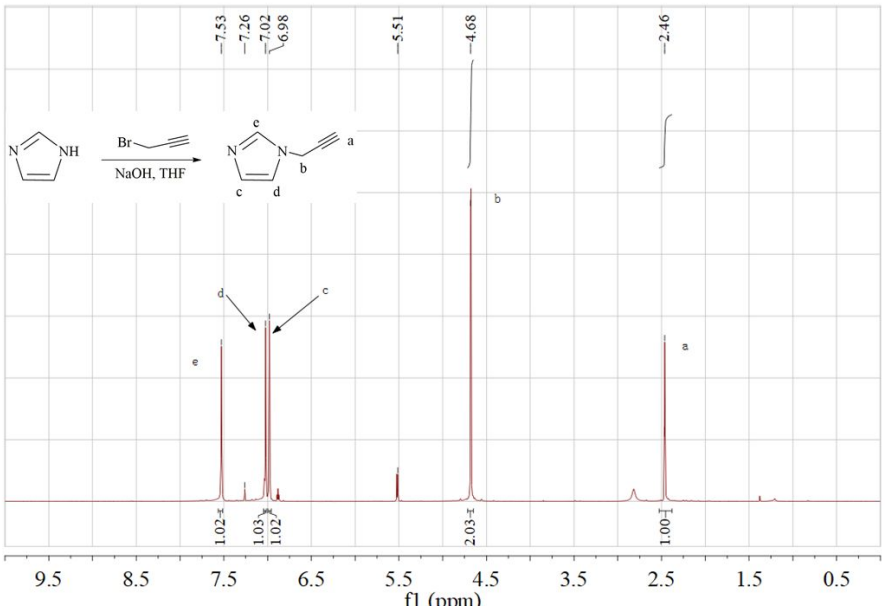

Figure S1. 600 MHz ^{1}H NMR spectrum of 1-propargylimidazole in $CDCl_3$.

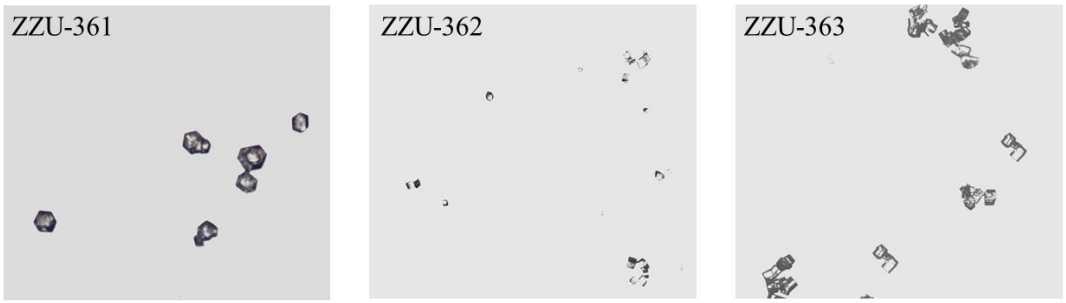

Figure S2. Photographs of as-synthesized ZZU-361, ZZU-362 and ZZU-363.

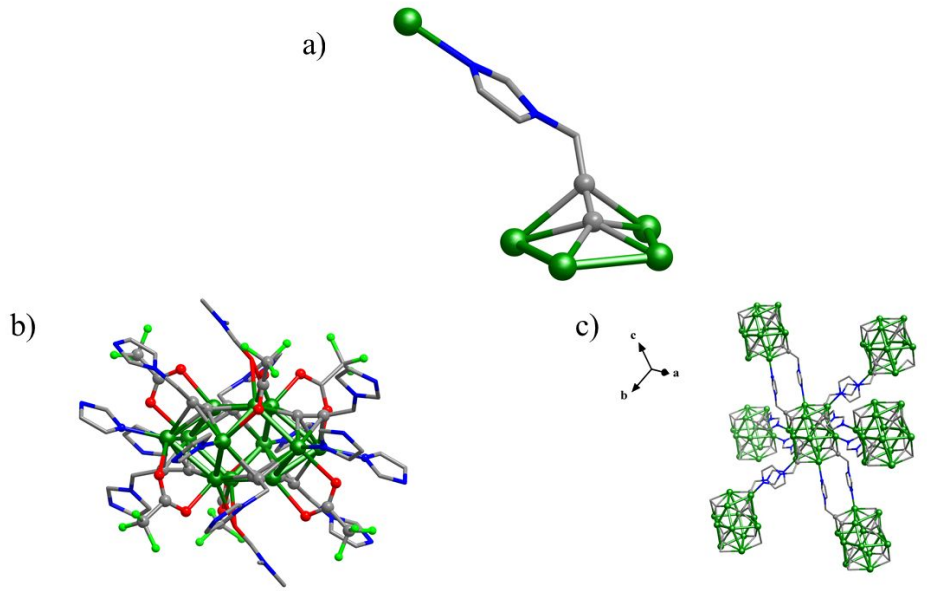

Figure S3. a) Coordination mode of alkyne groups in ZZU-361, b) the molecular structure and ligands of ZZU-361, and c) the linking pattern of the six surrounding Ag_{12} cores. All hydrogen atoms are omitted for clarity, and the Ag, C, N, F, and O atoms are shown in green, grey, blue, cyan, and red, respectively.

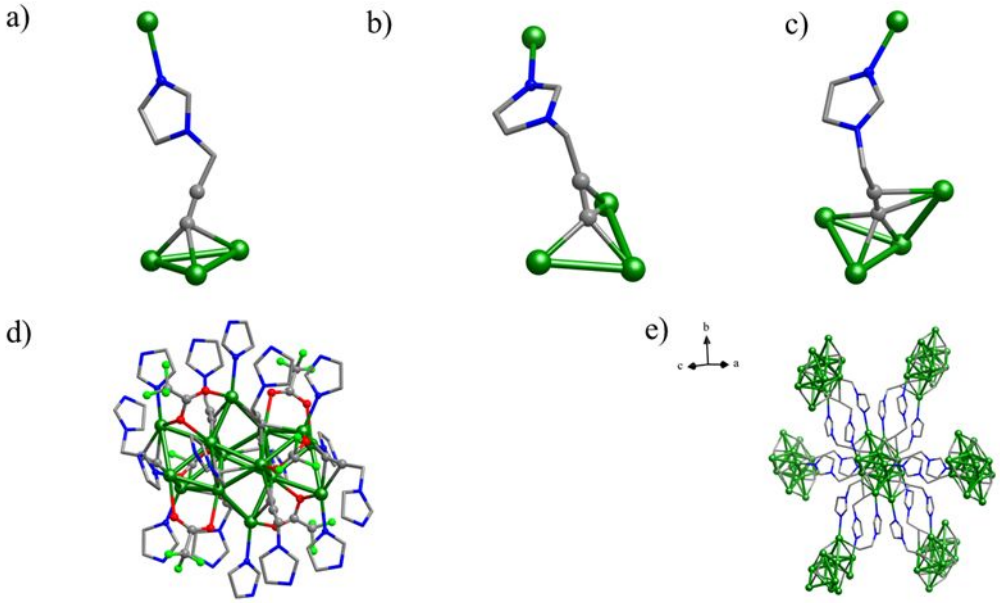

Figure S4. a), b), c) Coordination modes of the alkyne groups in ZZU-362, d) the molecular structure and ligands of ZZU-362, and e) the linking pattern of the six surrounding Ag14 cores. All hydrogen atoms are omitted for clarity, and the Ag, C, N, F, and O atoms are shown in green, grey, blue, cyan, and red, respectively.

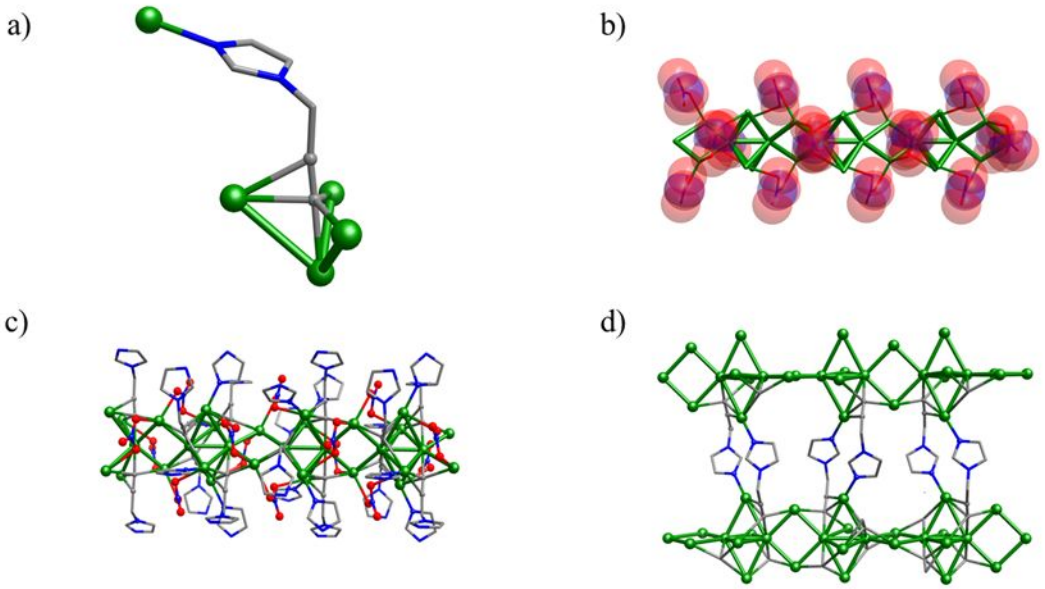

Figure S5. a) Coordination modes of the alkyne groups in ZZU-363, b) Coordination modes of NO_3^- in ZZU-363, c) the molecular structure and ligands of ZZU-363, and d) the linking pattern of each near two Ag_{1D} chains. All hydrogen atoms are omitted for clarity, and the Ag, C, N,and O atoms are shown in green, grey, blue, and red, respectively.

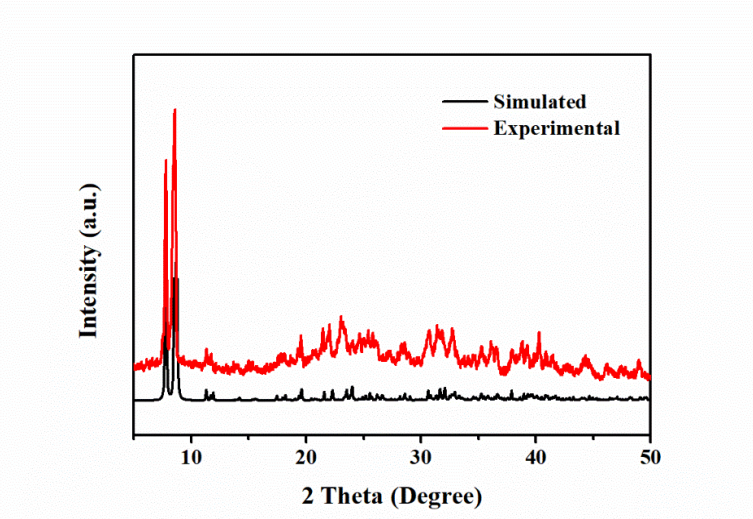

Figure S6. PXRD patterns of ZZU-361.

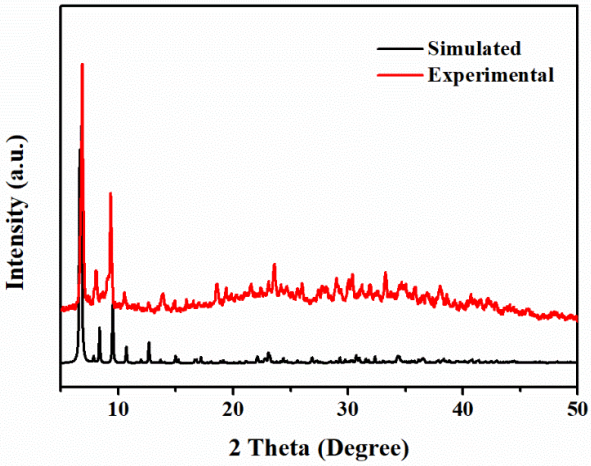

Figure S7. PXRD patterns of ZZU-362.

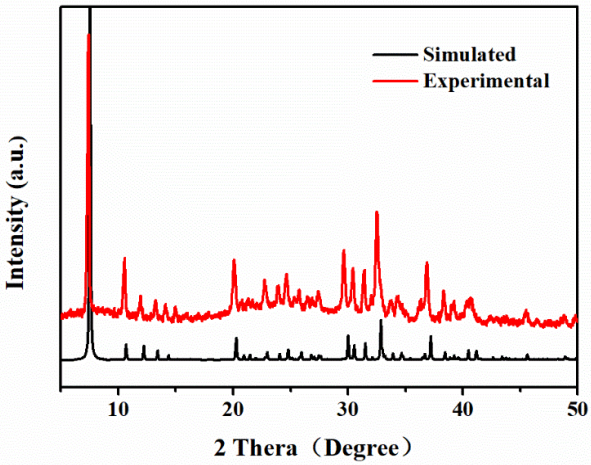

Figure S8. PXRD patterns of ZZU-363.

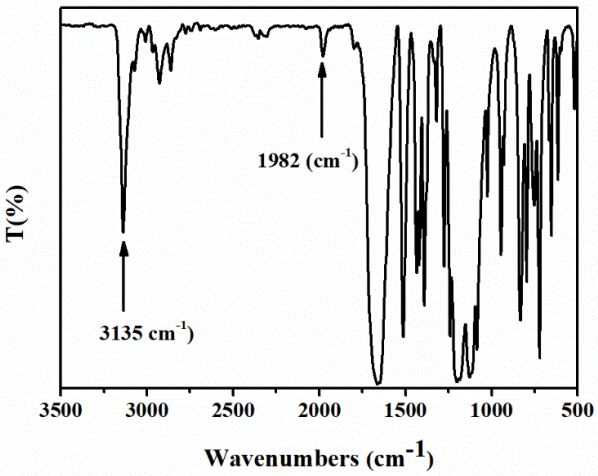

Figure S9. The FT-IR spectrum of ZZU-361.

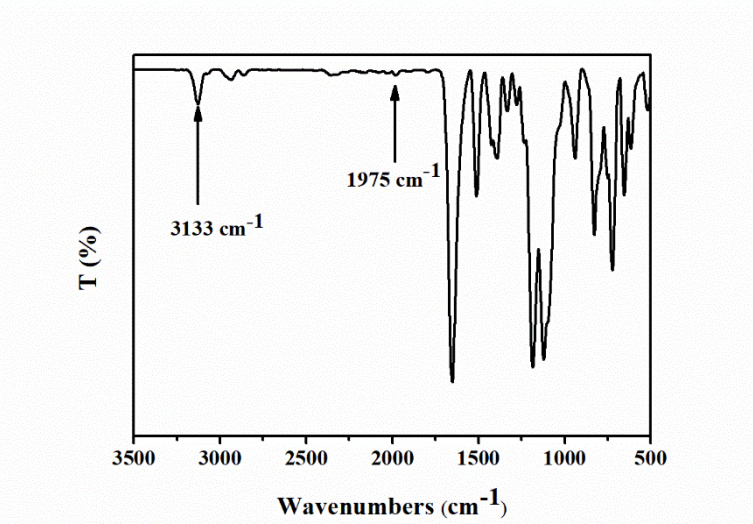

Figure S10. The FT-IR spectrum of ZZU-362.

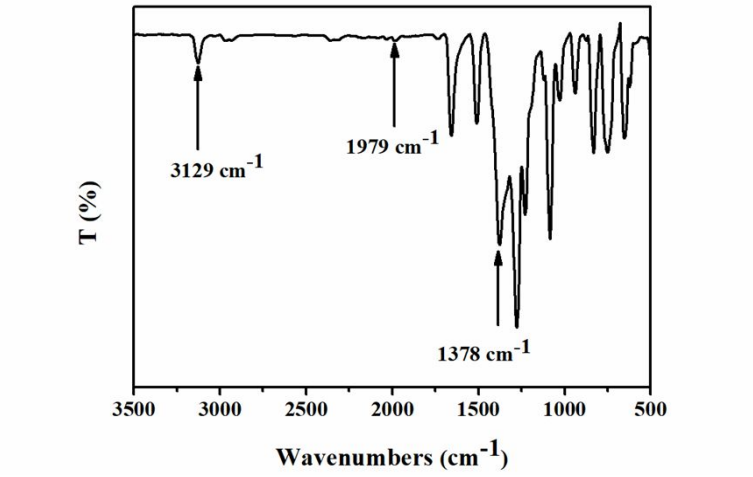

Figure S11. The FT-IR spectrum of ZZU-363

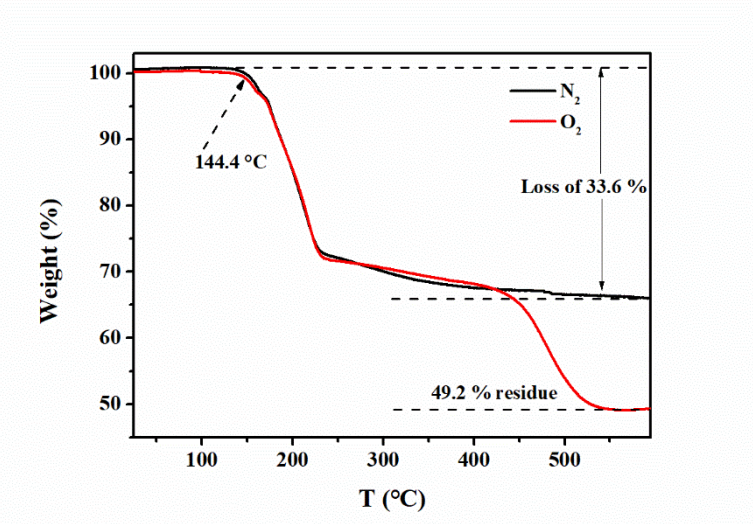

Figure S12. The TGA curves of ZZU-361.

For ZZU-361, only one major weight loss of 33.6% at a temperature range of 144.4 °C up to 200 °C was observed

under N_2 atmosphere, which was assigned to the loss of six CF_3COO^- auxiliary ligands and two DMF solvent molecules. Under O_2 atmosphere, the thermal degradation of ZZU-361 involved in two stages. The first stage was similar to that under N_2 atmosphere. The second stage at about 435.0 to 560.0 ºC can be regarded due to the oxidization of bridging ligands (PIm) and silver atom, where the left residue mass of 49.2% correspond to Ag_2O.

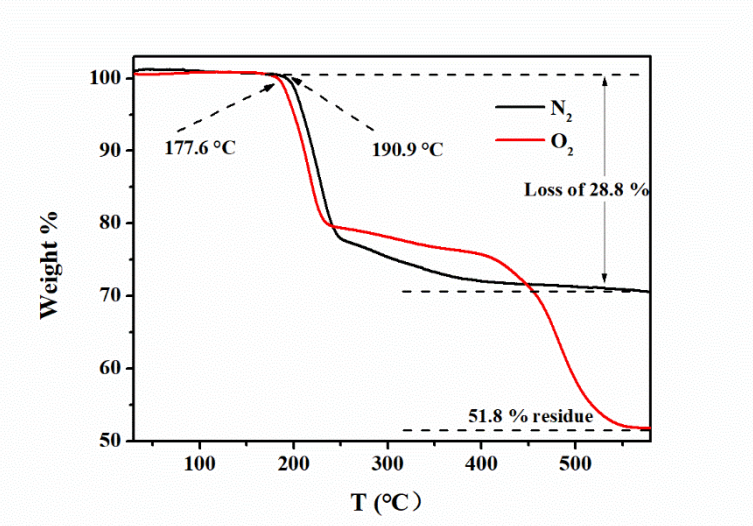

Figure S13. The TGA curves of ZZU-362.

As displayed in Figure S13, similar findings were found in the TG curves of ZZU-362. TGA showed a weight loss of 28.8% at ~190.9 °C - 230 °C under N_2 atmosphere, assigning to the loss of six CF_3COO^- auxiliary ligands collapse of the structure. As for the O_2 atmosphere, the degradation involved in two stages where the first stage (177.6 °C - 411.6 °C) corresponds to loss of CF_3COO^- ligands, followed by the decomposition of energetic ligand and oxidization of silver atom at much higher temperature (415.0 °C - 560.0 °C). And the residual mass of 51.8% was ascribed to Ag_2O.

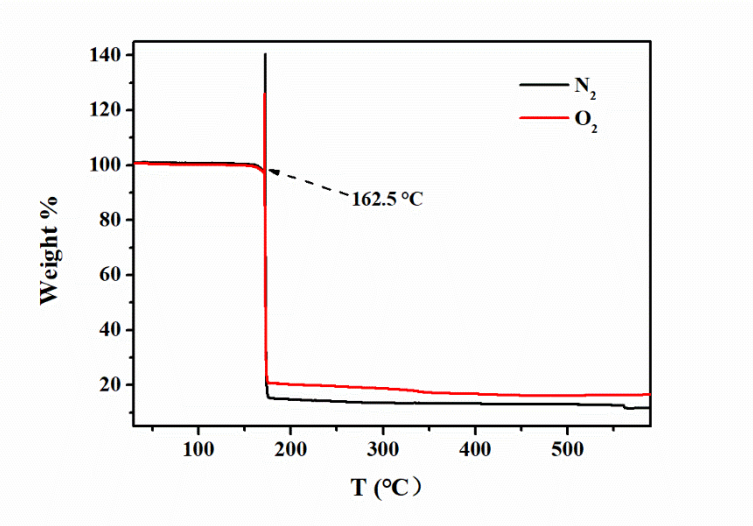

Figure S14. The TGA curves of ZZU-363.

For ZZU-363, the TGA curves were almost similar under both N_2 and O_2 atmosphere with a drastic energy release at 162.5 °C.

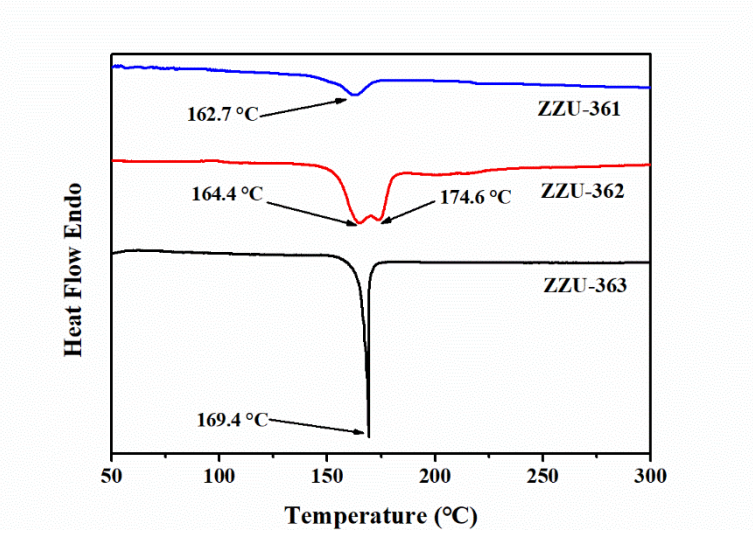

Figure S15. The DSC curves of ZZU-361, ZZU-362, ZZU-363.

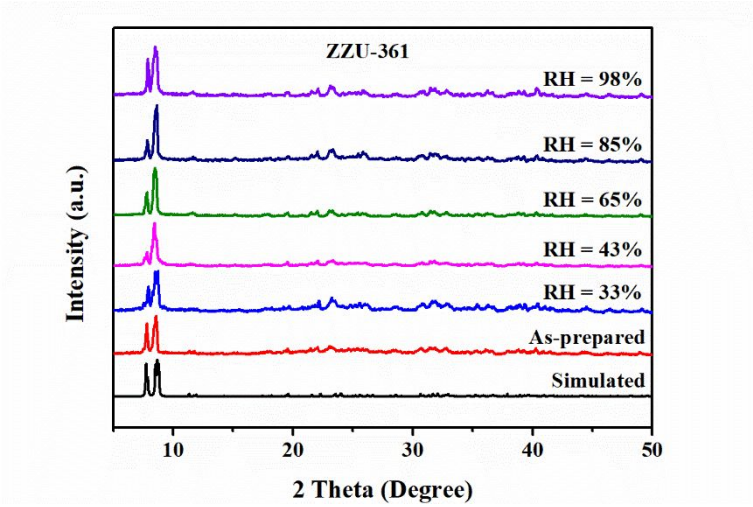

Figure S16. The PXRD patterns of ZZU-361 samples before and after exposing into differentRH conditions for three days.

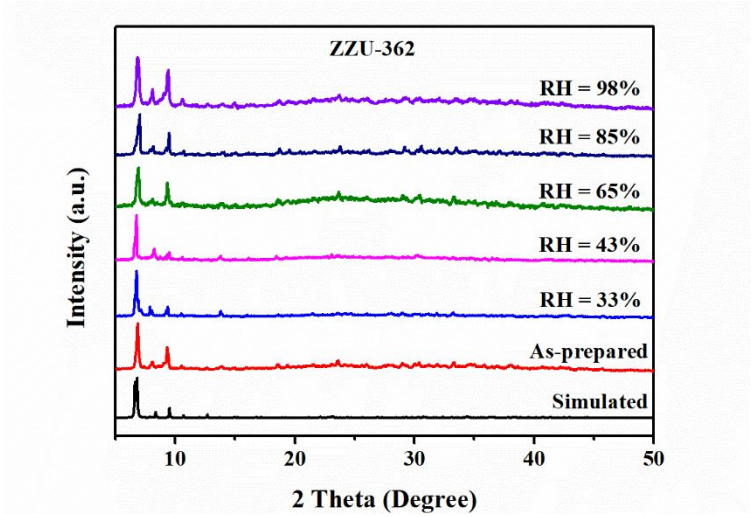

Figure S17. The PXRD patterns of ZZU-362 samples before and after exposing into different RH conditions for three days.

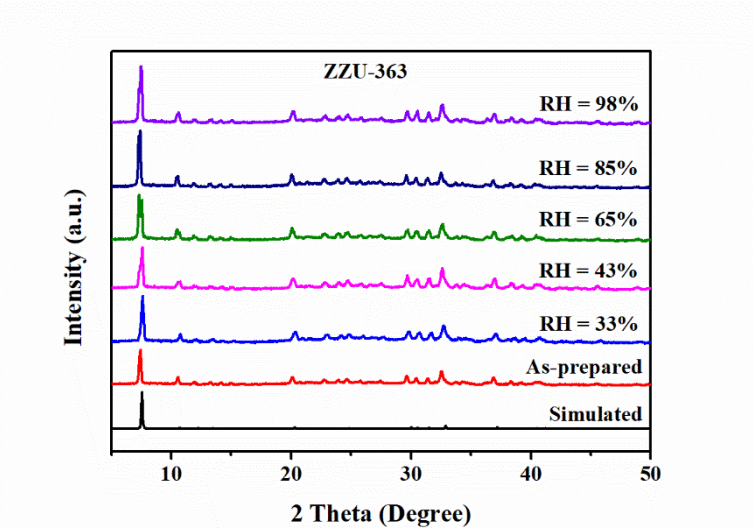

Figure S18. The PXRD patterns of ZZU-363 samples before and after exposing into different RH conditions for three days.

Section S4: Drop test procedure

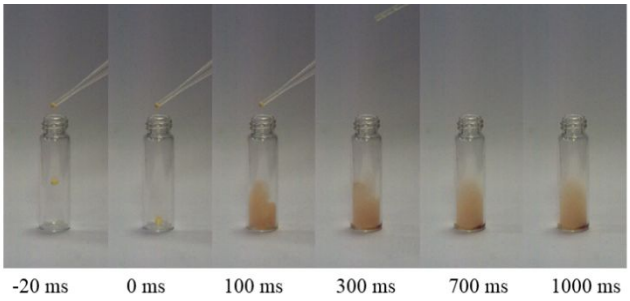

Figure S19. The hypergolic drop test of imidazole.

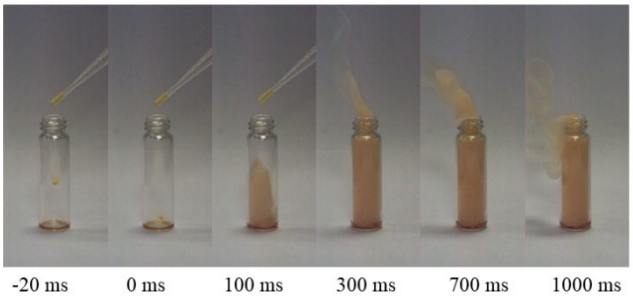

Figure S20. The hypergolic drop test of PIm.

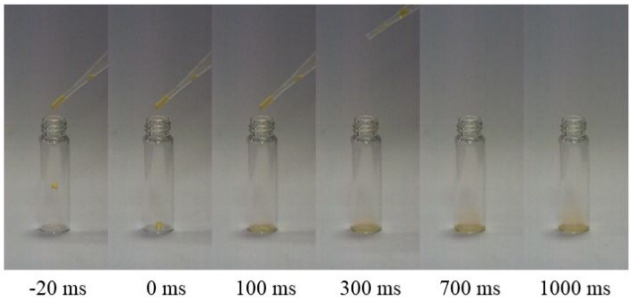

Figure S21. The hypergolic drop test of ^{t}BuC≡CAg.

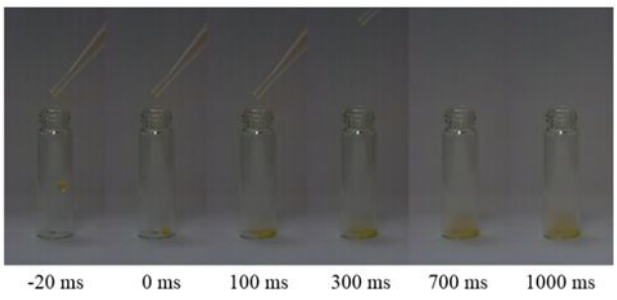

Figure S22. The hypergolic drop test of CF_3COOAg.

Figure S23. The hypergolic drop test of CF_3COOAg and PIm mixture.

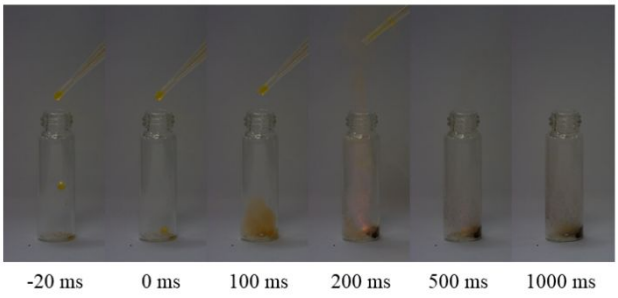

Figure S24. The hypergolic drop test of CF_3COOAg, ^{t}BuC≡CAg and PIm mixture.

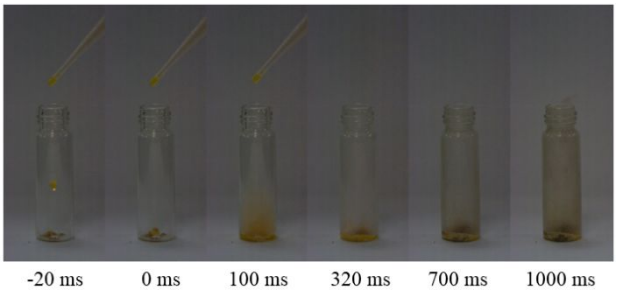

Figure S25. The hypergolic drop test of ^{t}BuC≡CAg and PIm mixture.

Section S5: Combustion Calorimetry

The combustion calorimetry experiment was conducted at a constant volume to measure the changes in internal energy.[3] Enthalpies were calculated from the internal energies measured by combustion calorimetry by taking into consideration the difference in the number of gaseous components (Δn) between the reactants and products of the combustion reactions.

$$\Delta_c U^{\theta}_m = \Delta_c H^{\theta}_m - \Delta nRT$$

The combustion reactions for each materials are provided below:

ZZU-361: $Ag_{12}C_{54}F_{18}N_{14}O_{14}H_{44(s)} + 56.5\ O_{2(g)} = 12\ AgF_{(s)} + 54\ CO_{2(g)} + 6\ HF_{(aq)} + 19\ H_2O_{(l)} + 7\ N_{2(g)}$ ($\Delta n = +4.5$)

ZZU-362: $Ag_{14}C_{64}F_{18}O_{14}N_{17}H_{51(s)} + 68.75\ O_{2(g)} = 14\ AgF_{(s)} + 64\ CO_{2(g)} + 4\ HF_{(aq)} + 23.45\ H_2O_{(l)} + 8.5\ N_{2(g)}$ ($\Delta n = +3.75$)

ZZU-363: $Ag_{16}C_{48}N_{24}O_{24}H_{40(s)} + 50\ O_{2(g)} = 8\ Ag_2O_{(s)} + 48\ CO_{2(g)} + 12\ N_{2(g)} + 20\ H_2O_{(l)}$ ($\Delta n = +10$)

Heat of formation was calculated by *Hess's* law using below equation (1).

$\Delta_f H^{\theta}_m = \Sigma \Delta_f H^{\theta}_m$ (product) - $\Delta_c H^{\theta}_m$ (1)

Section S6: Crystal Data and Structure Refinement

Data collection and reduction were performed using the CrysAlisPro program. The structure was solved by intrinsic phasing methods (SHELXT-2015)[4] and refined by full-matrix least squares on F^2 using *OLEX2*[5], which utilizes the SHELXL-2015 module[6].

Table S1. Crystal data and structure refinement for ZZU-361.

Identification code	ZZU-361
CCDC number	2083406
Empirical formula	$C_{48}H_{30}Ag_{12}F_{18}N_{12}O_{12}$
Formula weight	2749.47
Temperature (K)	200.00(10)
Crystal system	triclinic
Space group	*P-1*
a (Å)	12.01740(10)
b (Å)	13.6445(2)
c (Å)	13.6994(2)
α (°)	113.491(2)
β (°)	104.7130(10)
γ (°)	106.9600(10)
Volume (Å^3)	1786.42(5)
Z	1
Density (calculated) (Mg/m^3)	2.556
μ/mm^{-1}	26.809
F (000)	1304.0
Radiation	CuKα (λ = 1.54184)
Crystal size/mm^3	0.1 × 0.1 × 0.1
2 Theta range for data collection (°)	7.736 to 146.732
Index ranges	-14 ≤ h ≤ 14, -16 ≤ k ≤ 16, -17 ≤ l ≤ 16
Reflections collected	38152
Independent reflections	7047 [R_{int} = 0.0551, R_{sigma} = 0.0320]
Data/restraints/parameters	7047 / 72 / 557
Goodness-of-fit on F^2	1.044
Final *R* indices [I > 2sigma(I)]	R_1 = 0.0269, wR_2 = 0.0672
R indices (all data)	R_1 = 0.0289, wR_2 = 0.0683
Largest diff. peak and hole (e. Å^{-3})	1.29/-1.03

Table S2. Crystal data and structure refinement for ZZU-362.

Identification code	ZZU-362
CCDC number	2083405
Empirical formula	$C_{64}H_{51}Ag_{14}F_{18}N_{17}O_{14}$
Formula weight	3134.38
Temperature (K)	200.00(10)

Crystal system	monoclinic
Space group	$P2_1/c$
a (Å)	13.2636(6)
b (Å)	21.0964(8)
c (Å)	16.3979(9)
α (°)	90
β (°)	90.088(4)
γ (°)	90
Volume (Å^3)	4588.4(4)
Z	2
Density (calculated) (Mg/m^3)	2.269
μ/mm^{-1}	24.268
F (000)	2972.0
Radiation	CuKα (λ = 1.54184)
Crystal size/mm^3	0.05 × 0.05 × 0.05
2 Theta range for data collection (°)	6.828 to 132.986
Index ranges	-13 ≤ h ≤ 15, -24 ≤ k ≤ 18, -19 ≤ l ≤ 13
Reflections collected	21841
Independent reflections	7993 [R_{int}= 0.0744, R_{sigma}= 0.0863]
Data/restraints/parameters	7993 / 352 / 761
Goodness-of-fit on F^2	1.021
Final R indices [I > 2sigma(I)]	R_1= 0.1060, wR_2= 0.3047
R indices (all data)	R_1= 0.1410, wR_2= 0.3361
Largest diff. peak and hole (e. Å^{-3})	3.51/-1.73

Table S3. Crystal data and structure refinement for ZZU-363.

Identification code	ZZU-363
CCDC number	2083407
Empirical formula	$C_{48}H_{40}Ag_{16}N_{24}O_{24}$
Formula weight	3062.96
Temperature (K)	200.00(10)
Crystal system	tetragonal
Space group	*P4/ncc*
a (Å)	16.38990(10)
b (Å)	16.38990(10)
c (Å)	14.3453(2)
α (°)	90
β (°)	90
γ (°)	90
Volume (Å^3)	3853.56(7)
Z	2
Density (calculated) (Mg/m^3)	2.640
μ/mm^{-1}	32.541

F (000)	2880.0
Radiation	CuKα (λ = 1.54184)
Crystal size/mm^3	0.03 × 0.03 × 0.01
2 Theta range for data collection (°)	10.796 to 148.142
Index ranges	-12 ≤ h ≤ 19, -13 ≤ k ≤ 20, -13 ≤ l ≤ 17
Reflections collected	10460
Independent reflections	1925 [R_{int}= 0.0450, R_{sigma}= 0.0327]
Data/restraints/parameters	1925 / 0 / 128
Goodness-of-fit on F^2	1.127
Final R indices [I > 2sigma(I)]	R_1= 0.0316, wR_2= 0.0864
R indices (all data)	R_1= 0.0354, wR_2= 0.0895
Largest diff. peak and hole (e. Å^{-3})	0.56/-1.66

$R_1 = \Sigma||F_o|-|F_c||/\Sigma|F_o|$. $wR_2 = [\Sigma w(F_o^2-F_c^2)^2/\Sigma w(F_o^2)^2]^{1/2}$

Section S7: Theoretical Calculations

The density of states (DOS) and electrostatic potential (ESP) on the molecular van der Waals (vdW) surface were determined with the Vienna Ab initio Software Package (VASP 5.3.5) code under the Perdew–Burke–Ernzerhof (PBE) generalized gradient approximation and the projected augmented wave (PAW) method.[7-10] The cut-off energy for the plane-wave basis set was set to 400 eV. The Brillouin zone of the surface unit cell was sampled by Monkhorst–Pack (MP) grids for structure optimizations.[11]

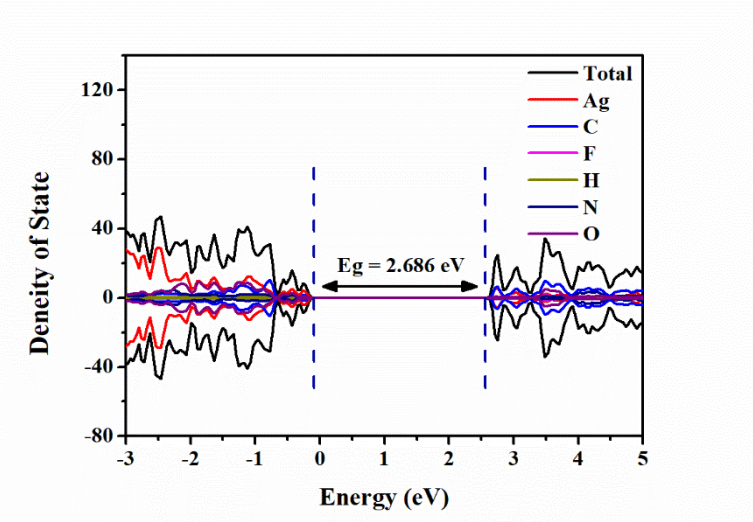

Figure S26. Total and partial density of states (DOS) of ZZU-361.

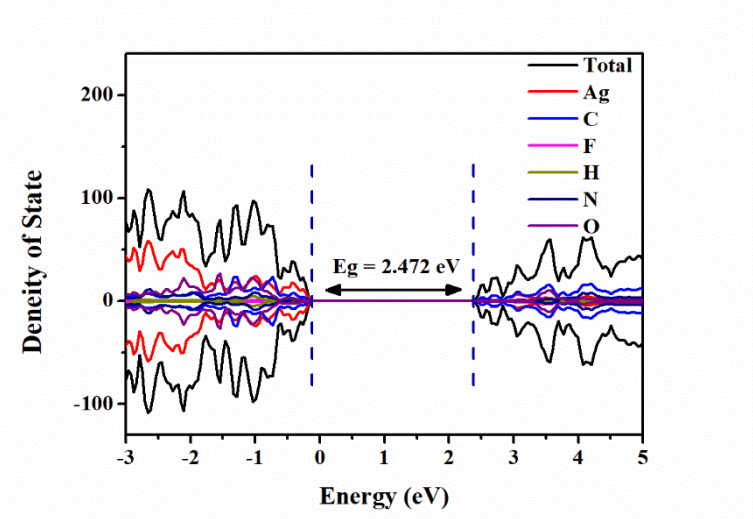

Figure S27. Total and partial density of states (DOS) of ZZU-362.

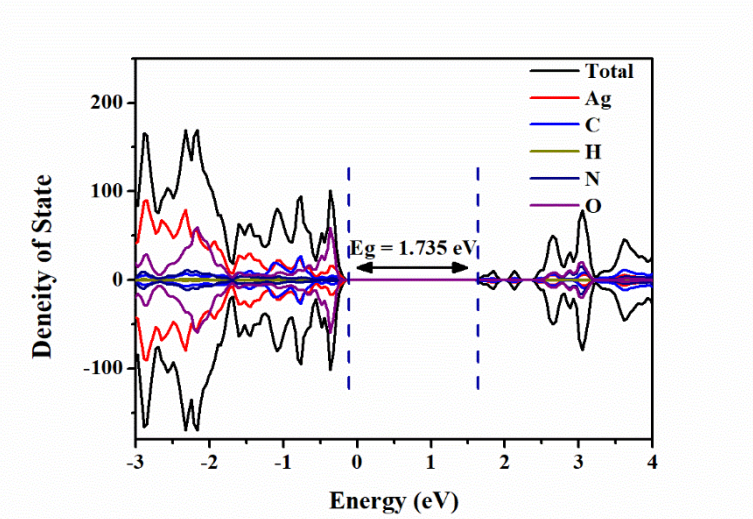

Figure S28. Total and partial density of states (DOS) of ZZU-363.

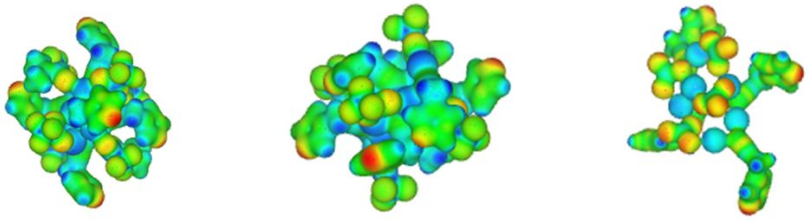

ZZU-361 ZZU-362 ZZU-363

Figure S29. ESP-mapped vdW surface of ZZU-361, ZZU-362 and ZZU-363 at the vasp. The surface local minima and maxima of ESP are represented as red and blue points, respectively.

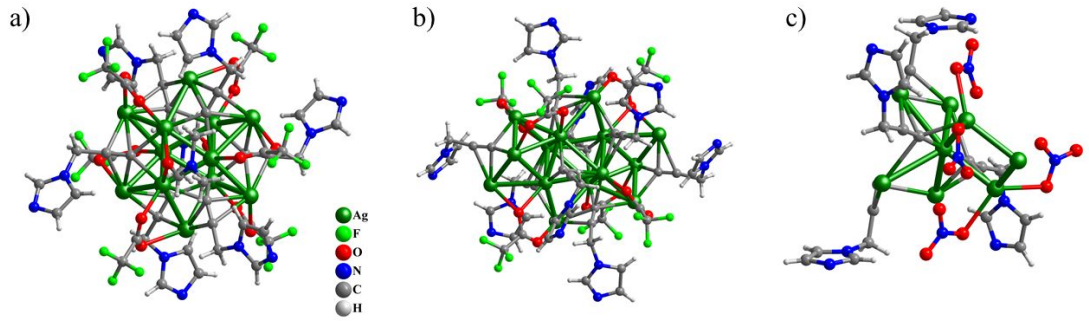

$Ag_{12}(CF_3COO)_6(PIm)_6(DMF)_2$ $Ag_{14}(CF_3COO)_6(PIm)_8$ $Ag_8(NO_3)_4(PIm)_4$

Figure S30. Three reaction models was chosen for catalytic mechanism. The structures of ZZU-361, ZZU-362, and ZZU-363 were represented by $Ag_{12}(CF_3COO)_6(PIm)_6(DMF)_2$, $Ag_{14}(CF_3COO)_6(PIm)_8$, and $Ag_8(NO_3)_4(PIm)_4$, respectively.

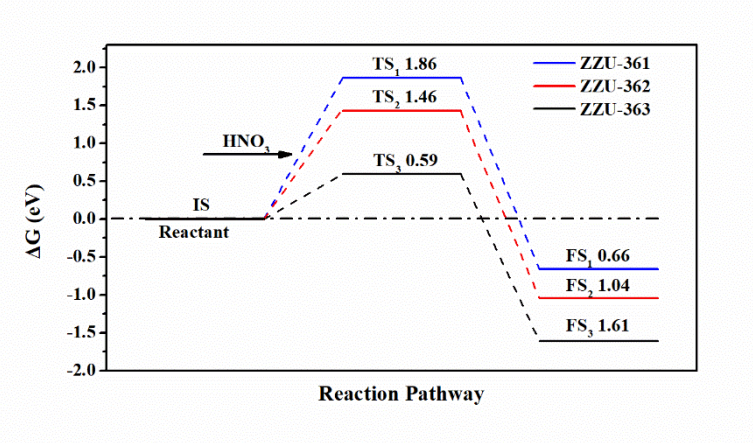

Figure S31. Calculated free energy diagram of ZZU-361, ZZU-362 and ZZU-363 reacting with HNO_3 molecule at 2000 K.

References:

1. J. Wang, H. T. Zhu, S Chen, Y. Xia, D. P. Jin, Y. F. Qiu, Y. X. Li, Y. M. Liang, Electrophilic Cyclization of Aryl Propargylic Alcohols: Synthesis of Dihalogenated 6,9-Dihydropyrido[1,2-a]indoles via a Cascade Iodocyclization. *J. Org. Chem.* **2016**, *81*, 10975-10986.
2. W. D. Liu, J. Q. Wang, S. F. Yuan, X. Chen, Q. M. Wang, Chiral Superatomic Nanoclusters Ag_{47} Induced by the Ligation of Amino Acids. *Angew. Chem. Int. Ed. Engl.* **2021**, *60*, 11430-11435.
3. X. C. Yang, S. Chen, S. Gao, H. Li, Q. Shi, CONSTRUCTION OF A ROTATING-BOMB COMBUSTION CALORIMETER AND MEASUREMENT OF THERMAL EFFECTS. *Instrum. Sci. Technol.* **2002**, *30*, 311-321.
4. M. H. So, V. A. L. Roy, Z. X. Xu, S. S. Chui, M. Y. Yuen, C. M. Ho, C. M. Che, Controlled Self-Assembly of Functional Metal Octaethylporphyrin 1 D Nanowires by Solution-Phase Precipitative Method. *Chem. Asian J.* **2008**, *3*, 1968-1978.
5. O. V. Dolomanov, L. J. Bourhis, R. J. Gildea, J. A. K Howard, H. Puschmann, *OLEX2*: a complete structure solution, refinement and analysis program. *J. Appl. Cryst.* **2009**, *42*, 339-341.
6. G. M. Sheldrick, *SHELXT* - Integrated space-group and crystal-structure determination. *Acta Cryst.A* **2015**, *71*, 3-8.
7. J. P. Perdew, K. Burke, M. Ernzerhof, Generalized Gradient Approximation Made Simple *Phys. Rev. Lett.* **1996**, *77*, 3865-3868.
8. B. Hammer, L. B. Hansen, J. K. Nørskov, Improved adsorption energetics within density-functional theory using revised Perdew-Burke-Ernzerhof functionals. *Phys. Rev. B.* **1999**, *59* , 7413-7421.
9. P. E. Blöchl, Projector augmented-wave method. *Phys. Rev. B.* **1994**, *50*, 17953-17979.
10. G. Kresse, D. Joubert, From ultrasoft pseudopotentials to the projector augmented-wave method. *Phys. Rev. B.* **1999**, *59*, 1758-1775.
11. H. J. Monkhorst, J. D. Pack, Special points for Brillouin-zone integrations. *Phys. Rev. B.* **1976**, *13*, 5188-5192.